Journal of Inorganic and Organometallic Polymers and Materials (2021) 31:2791–2805
https://doi.org/10.1007/s10904-021-01910-9

Functionalize Aramid Fibers with Polydopamine to Possess UV Resistance

Mingzhuan Li[1,2] · Kan Cheng[1,2] · Caihong Wang[1,2] · Shengjun Lu[1,2]

Received: 13 November 2020 / Accepted: 20 January 2021 / Published online: 15 February 2021

Abstract

The paper designs a novel and green method to improve the surface activity and UV resistance of aramid fibers. The fibers were treated by UV radiation and then functionalized with dopamine, reaching the result that a dense and uniform polydopamine (PDA) was coated on the surface of the fibers. The surface morphology, chemical structure, aggregation structure and wettability, UV resistance and mechanical properties of the aramid fibers were characterized by SEM, AFM, ATR-FTIR, XPS, XRD, UV absorption spectroscopy, contact angle and mechanical properties tests. The results showed that the dopamine was successfully coated on the surface of the fibers, and the chemical structure of the surface of the functionalized fiber changed, but the aggregation structure did not change. The surface activity and UV resistance of the functionalized fiber significantly improved. Compared with untreated aramid fibers, after the fibers were radiated under UV treatment for one week, the retention of strength and elongation at break of the functionalized fiber with dopamine increased nearly 20%, respectively. These results demonstrated that PDA layer could significantly improve the surface properties of aramid fibers and play a key role in protecting the cortical structure of the fibers. So far, the researches on improving the surface activity and UV resistance of fibers by functionalization with dopamine have rarely been reported, so the method is novel and worth for further studying.

Keywords Aramid fiber · Dopamine · Functionalization · Surface activity · UV resistance

1 Introduction

Aramid fiber is one of the organic high-performance fibers. Aramid fiber combines high strength, thermal stability and chemical stability with low density [1–4]. Due to its unique excellent properties, it is widely used as the reinforcement material in the advanced polymer composites [5–8]. Furthermore, aramid fiber reinforced polymer composites were applied in military applications, aerospace, automotive, electronic products, industry and other fields [9–13], and were obtained the wide attention from researchers.

However, the aramid fiber has poor surface activity [5, 14–16] and UV resistance [17–20], which severely limits the applications of the aramid fiber. Solving these two bottlenecks and maintaining the excellent mechanical properties of the aramid fiber are a huge challenge, and the researchers have conducted a lot of researches on this. Zhang [21] prepared grafted Kevlar fibers (HSi-g-KF) with improving surface activity and UV resistance by in-situ synthesis of hyperbranched polysiloxanes with double bonds and epoxy groups on the Kevlar fibers. Zhou [17] improved the surface activity and UV resistance of the fibers with green layer-by-layer (LBL) self-assembly technology by alternately self-assembling SiO_2 and MgAlFe layered double hydroxide (LDH) on the surface of the aramid fiber. Cai [22] synthesized a UV absorber with strong UV absorption and high surface activity by sequentially forming nano-layered boron nitride (tBN) and PDA layer on the CeO_2 core (PDA@tBN@CeO_2). Zhu [23] prepared a novel surface-modified aramid fiber with hyperbranched polysiloxane (His)-$Ce_{0.8}Ca_{0.2}O_{1.8}$ hybrid coating by in-situ method, which could improve the UV resistance and the surface activity of fibers. These methods have complicated steps or harsh condition.

✉ Shengjun Lu
sjlu@gzu.edu.cn

1 College of Materials and Metallurgy, Guizhou University, Guiyang 550025, Guizhou, China

2 National Engineering Research Center for Compounding and Modification of Polymeric Materials, Guiyang 550014, Guizhou, China

In 2007, Lee [24] was inspired by the viscous protein from the mussels and first discovered polydopamine polymer and found that polydopamine has strong adhesion and could adhere to almost any surface. Since its inception, polydopamine has been wide studies and applications [25, 26] because of its strong adhesion properties [27]. In the paper, a simple and green method was used to improve the surface activity and UV resistance of aramid fibers. Firstly, the aramid fiber was treated by UV radiation to activate and roughen its surface, and then the fiber was functionalized in dopamine solution to obtain a dense and uniform PDA coating on the fiber by utilizing the adhesion properties of the PDA.

The paper focuses on the surface activity and UV resistance of the functionalized fibers with dopamine. There is no report on the detailed analysis of the UV resistance of PDA coatings. In this paper, the mechanism and reasons of improving the UV resistance of PDA coating of aramid fibers are clearly elaborated. This paper provides a novel method for improving the UV resistance of aramid fiber, which has an important significance for prolonging the service life of aramid fiber, and has an important influence on broadening the applications of aramid fiber.

2 Experimental

2.1 Experimental Materials

Aramid fiber (Kevlar-29): Model 956, specification 1500D, linear density 1670dtex, DuPont, USA. 3-Hydroxytyramine Hydrochloride: Grade Reagent (RG), purity 99%+, molecular weight 189.64, Adamas. Tris (Tris reagent): grade ACS, purity 99%, molecular weight 121.14, Adamas. Ethanol (ethyl alcohol): density (20 °C) is 0.789–0.791 g/ml, Analytical Grade (AR), content ≥ 99.7%, Tianjin Fuyu Chemical.

2.2 Cleaning the Aramid Fiber

The aramid fiber was cut into short fibers about 3–5 cm, ultrasonically cleaned in absolute ethanol for 3 h, then washed five times with deionized water, finally dried in a blast oven at 60 °C for 10 h, and the aramid fiber was taken out for later use.

2.3 UV Radiation Treatment of Aramid Fiber

The aramid fiber was placed in an ultraviolet aging test chamber (model: GM-UVA-2130, Shenzhen Guangmai Instrument Equipment Co., Ltd.) for 0 h, 10 h, 20 h, 30 h and 40 h, respectively, to obtain treated aramid fiber with ultraviolet radiation. UV-0 h, UV-10 h, UV-20 h, UV-30 h and UV-40 h were marked separately.

2.4 Preparation of KF-UV-PDA

The dopamine hydrochloride was dissolved in deionized water to prepare a dopamine solution with a concentration of 2.0 g/L. The Tris–HCl reagent was added to the dopamine solution, and the pH of the solution was adjusted to 8.5 [24] with a pH meter (Metteler Toledo FE-20). In general, a 2.0 g/L dopamine solution and a 1.2 g/L Tris solution can bring the solution to a predetermined pH [28, 29]. The ultraviolet radiation-treated aramid fiber was placed in prepared dopamine solution, allowed to stand at room temperature for 24 h, and then placed in a 40 °C blast oven for 24 h. Finally, the obtained KF-UV-PDA fiber was used for the subsequent test.

3 Characterization

3.1 Scanning Electron Microscopy Test (SEM)

The surface morphology of the aramid fiber was observed with the scanning electron microscope (Quanta FEG 250, FEI Instruments, USA).

3.2 Atomic Force Microscopy Test (AFM)

The surface of the aramid fiber was scanned in a tapping mode using the German Bruker's Dimension Icon. All data were passed through the NanoScope Analysis software. A second-order leveling was performed to ensure the images at the same height, thereby eliminating errors caused by changes in angle.

3.3 Transmission Electron Microscope Test (TEM)

The aramid fiber was tested by a transmission electron microscope of JEM-1230 by JEOL to obtain the appearance and the thickness of the PDA coating.

3.4 Infrared Analysis (ATR-FTIR)

A bundle of fibers was placed on a Fourier infrared spectrometer (Nicolet iS50, American Thermo Fisher Scientific) testing platform, and the aramid fiber was tested in attenuated total reflection infrared (ATR-FTIR) mode with a spectral resolution of 2 cm^{-1}, the wave number range is 600 ~ 4000 cm^{-1}, the number of scans is 32 times.

3.5 X-ray Photoelectron Spectroscopy (XPS)

The surface elements and their contents of the aramid fiber were analyzed by X-ray photoelectron spectroscopy

(K-Alpha+, Thermo Fisher Scientific, USA). The X-ray source used in the experiment was an Al Kα (Mono Al Kα) with an energy of 1486.6 eV, 6 mA × 12 kV, a beam spot size of 400 μm, an operating vacuum of $2 \times 10^{-}7$ mba in the analysis chamber, and a CAE mode in the scanning mode. When the fiber was scanned in full spectrum, the energy was 100 eV and the step size was 1 eV. When the fiber was performed in narrow spectrum, the energy was 30 eV and the step size was 0.1 eV. And each sample was tested for five times.

3.6 X-ray Diffraction Analysis (XRD)

The structural of fibers were tested with using an X-ray diffractometer (X PertPower, Panaco X-Ray Analytical Instruments, Netherlands). The experiment used a Cu target with the range of 5°–90° and the scanning speed was 10°/min.

3.7 Contact Angle Test

The aramid woven fabric was functioned with PDA with the same method as the method of the functioned fiber. The contact angle test was carried out on the aramid woven fabric by the contact angle measuring instrument (Model DSA25, KRÜSS, Germany) to test the wetting ability of the fiber. The liquid used in the experiment was deionized water.

3.8 UV Absorption Spectroscopy

UV–visible spectrophotometer (Lambda 950 double-beam type, PerkinElmer, USA) was used to test the absorption capacity of the ultraviolet light of the aramid fiber. The testing wavelength was 200 ~ 800 nm.

3.9 Mechanical Properties Analysis

XQ-1C fiber strength extensometer (Shanghai Xinmao Instrument Co., Ltd.) was used to test the tensile properties of aramid fiber, the tensile rate was 10 mm/min, and the clamping distance was 20 mm. 30 valid data were conducted for each sample.

3.10 KF-UV (40 h)-Ultrasonic Treatment of PDA Fibers

Ultrasonic treatment (JP-020, ultrasonic power 120 W, ultrasonic frequency 40KHz, Shenzhen Jiemeng Cleaning Equipment Co., Ltd.) was used to get ultrasonic KF-UV(40 h)-PDA fiber. And the adhesion property of the dopamine coating was then evaluated by observing the SEM image of the surface of the fiber.

4 Results and Discussion

Figure 1 showed the schematic diagram that the aramid fiber was modified under UV radiation and functionalized by dopamine. After the aramid fiber was under UV radiation, the surface of the fiber became rough and could destroy the amide bond in molecular chain of the surface, so a small amount of carboxyl functional group was obtained by the reaction of oxidation [30]. Dopamine can self-polymerize on the surface of the fiber and dopamine was rich in phenolic hydroxyl functional groups. The carboxyl functional group on the surface could be esterified with the phenolic hydroxyl group and the interaction between π–π occurred. Under the

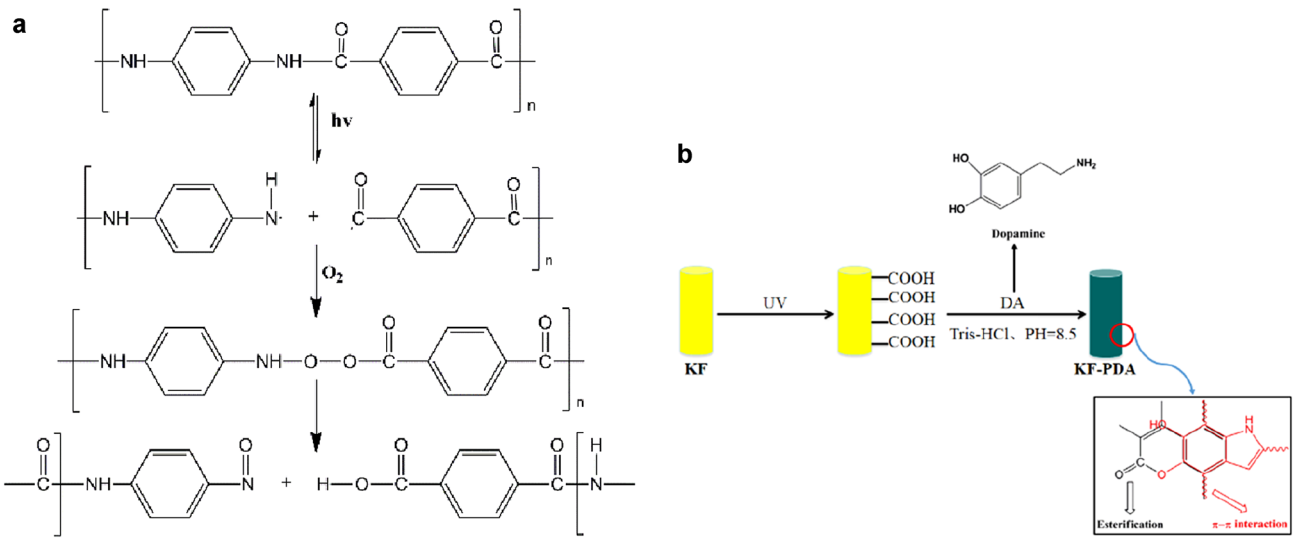

Fig. 1 Schematic diagram of aramid fiber undergoing UV radiation (**a**) and dopamine functionalization (**b**)

dual interaction, the PDA coating could tightly adhere on the aramid fiber and increase the coverage of the coating.

4.1 Scanning Electron Microscopy (SEM) Test

Figure 2 represented scanning electron micrographs of the untreated fiber and functionalized fiber with PDA. It could be clearly seen from the figure that the surface of KF was very smooth and clean, and there were no cracks and deposits on the surface. However, the surface of KF-UV-PDA had dopamine coating and small particles, which made the surface uneven and increased the roughness of the surface. This is beneficial to improve the surface activity and interfacial adhesion of the aramid fiber. What's more, as the time of UV irradiation increased, the PDA coating became dense. Especially when the UV radiation was 40 h, the coating of the KF-UV(40 h)-PDA was the most dense. This indicated that the modified aramid fiber with UV irradiation was more beneficial to the adhesion of dopamine on its surface. From the pictures of the KF and KF-UV(40 h)-PDA samples, it

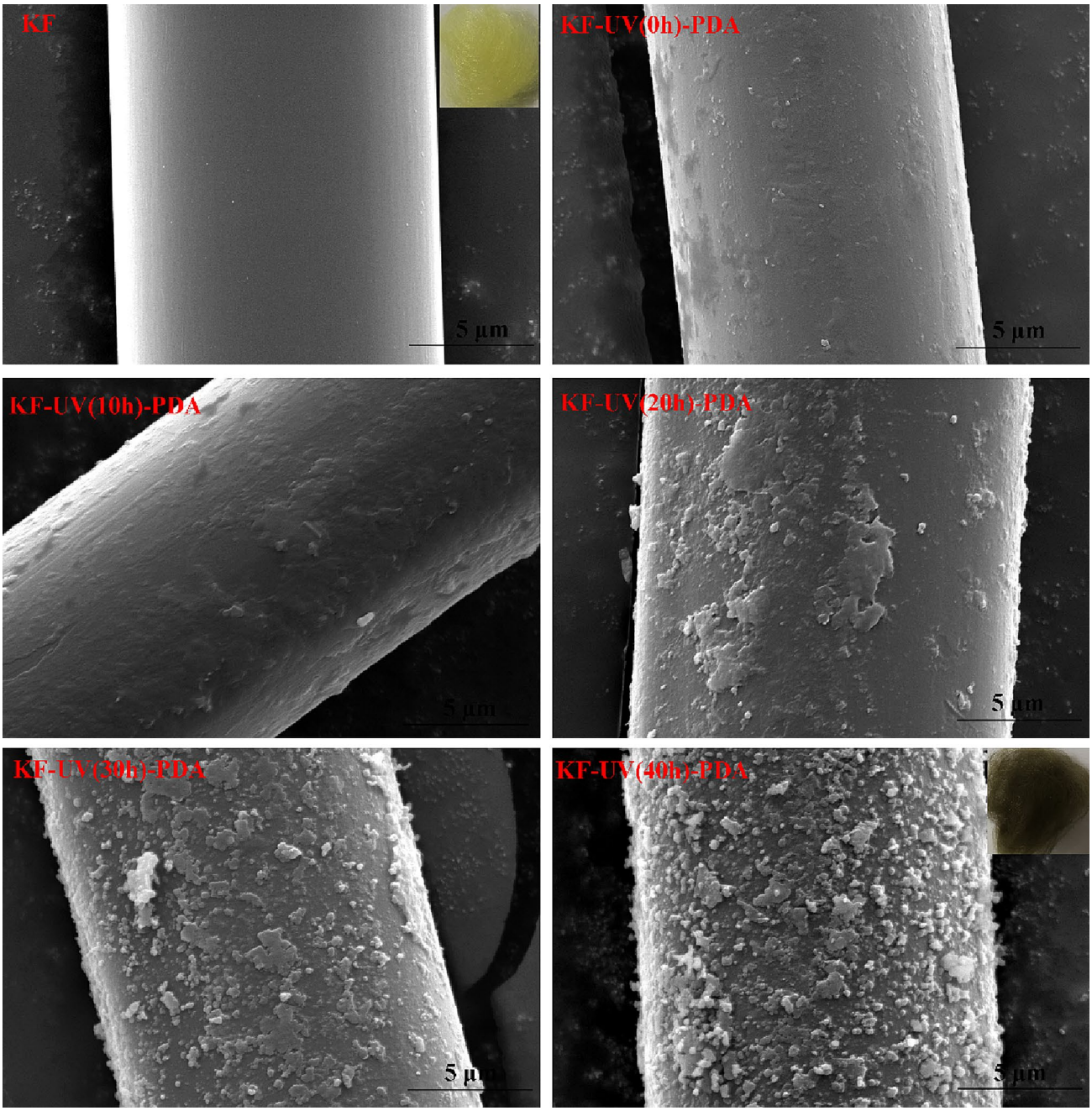

Fig. 2 SEM of the untreated fiber and functionalized fiber with dopamine

was apparent that the fiber was significantly darkened by the functionalization with dopamine, which also indicated that the PDA was successfully coated on the aramid fiber.

4.2 Atomic Force Microscopy (AFM) Test

Figure 3 showed the surface topography of the aramid fiber using a tapping mode to strike the surface with a probe tip in a vibrating state to obtain an AFM image of the aramid fiber morphology. Figure 3a showed the atomic force microscopy of the untreated aramid fiber. It can be clearly seen from the figure that the surface of the aramid fiber was very smooth and clean, which is confirmed by the results of scanning electron microscopy. It can be clearly seen from the phase diagram of Fig. 3a–f that compared with the aramid fiber, the surface of the dopamine functionalized fiber has a different crystal phase, which is caused by the dopamine plating. And as the UV irradiation time increased, the thickness of the dopamine coating increased and became denser. Especially for the KF-UV(40)-PDA sample, the dense polydopamine coating on the surface of the aramid fiber can be clearly seen, which fully demonstrated that the dopamine was successfully plated on the fiber. It can be seen from Table 1 that the root mean square roughness (Rq) and the arithmetic mean roughness (Ra) of the untreated aramid fiber were small, 10.7 nm and 7.6 nm, respectively. But as the UV radiation time increased, the value of (Rq) and (Ra) of the functioned fiber with dopamine functionalization tended to increase overall. Based on the results of AFM and SEM, the coating density of KF-UV(40 h)-PDA samples was the best. The next parts selected KF-UV(40 h)-PDA to represent the performance of KF-UV-PDA fibers.

4.3 Transmission Electron Microscope (TEM) Test

Figure 4 represented the transmission electron micrograph and the thickness of the KF-UV(40 h)-PDA sample. It was evident from Fig. 4a and b that there was a uniform and dense PDA coating on the surface of the aramid fiber. The thickness of the PDA coating was measured by the Nano Measurer test software. The thickness was tested at 50 various points, and the data distribution of the thickness of the PDA layer was as shown in Fig. 4c. From the date, we got the result that the average thickness of the PDA layer was about 107 nm.

4.4 Infrared Analysis (ATR-FTIR)

Figure 5 represented the infrared characteristic absorption peaks of aramid fiber, modified fiber under UV radiation and functionalized aramid fiber with dopamine. Among them, Fig. 5a showed the infrared spectrum of the KF-UV fiber obtained under UV treatment. It can be seen from Fig. 5a that the absorption peak at 1715 cm^{-1} represented the cleavage of the amide bond and the production of the carboxylic acid group. At 1637 cm^{-1}, there was a strong carbonyl group C=O absorption peak, (belonging to the class I absorption peak of amide), and the peak intensity of the C=O peak increased with the increase of UV irradiation time; the NH peak at 1538 cm^{-1} also increased with the increase of UV radiation, which indicated that the C=O and NH group between adjacent molecular chains was broken [30]. The results can be attributed to the breakage of the fiber molecular chain and the oxidation of the edge groups during UV irradiation [31]. In order to confirm the chemical structure of the coating, the functionalized aramid fiber with dopamine (KF-UV-PDA) was tested by infrared test, and the results were shown in Fig. 5b. It can be seen from Fig. 5b that a bending vibration absorption peak of hydroxyl group (–OH) appeared at 1223 cm^{-1}, which indicated that dopamine was successfully plated on the surface of the aramid fiber, and the intensity of this peak was in accordance with the time of UV radiation. That was to say, as the UV radiation time increased, the dopamine was more likely to adhere to the aramid fiber. At 1611 cm^{-1}, a characteristic ring vibration absorption peak attributed to the aromatic ester [32], which was most likely due to the reaction of the C=O group produced under UV radiation on the fibers with the phenolic hydroxyl in dopamine, which further demonstrated that UV radiation could produce carboxyl functional groups on the aramid fibers.

4.5 X-ray Photoelectron Spectroscopy (XPS)

Figure 6 showed the XPS results of untreated aramid fibers, modified fiber under UV radiation and functionalized aramid fiber with dopamine. Figure 6a–f showed the XPS diagram of untreated aramid fiber and UV radiated aramid fiber. It can be concluded from Fig. 6a and Table 2 that: the ratio of N/C and the ratio of O/C of the KF was 0.10, 0.17, respectively; while the ratio of N/C and the ratio of O/C of the KF-UV(40 h) fiber was 0.05, 0.21, respectively. These results indicated that compared with KF, the ratio of N/C of KF-UV(40 h) fiber decreased, but the ratio of O/C increased. The reason was very likely that UV radiation destroyed the amide bond in the molecular chain of the aramid fiber, and during the UV irradiation, the oxidation reaction on aramid fiber occurred, so that the content of N element decreased and the content of the containing oxygen group on the surface of the fiber increased [31, 33, 34]. From the C1s spectrum 6(b–f), it can be found that: compared with untreated KF, the fiber after UV irradiation increased the peak of the –COO–(288.5 eV) group because the surface of fiber was oxidized to produce carboxy after UV irradiation. And the content of the –COO– group increased as the UV irradiation time increased, which indicated that the content of the

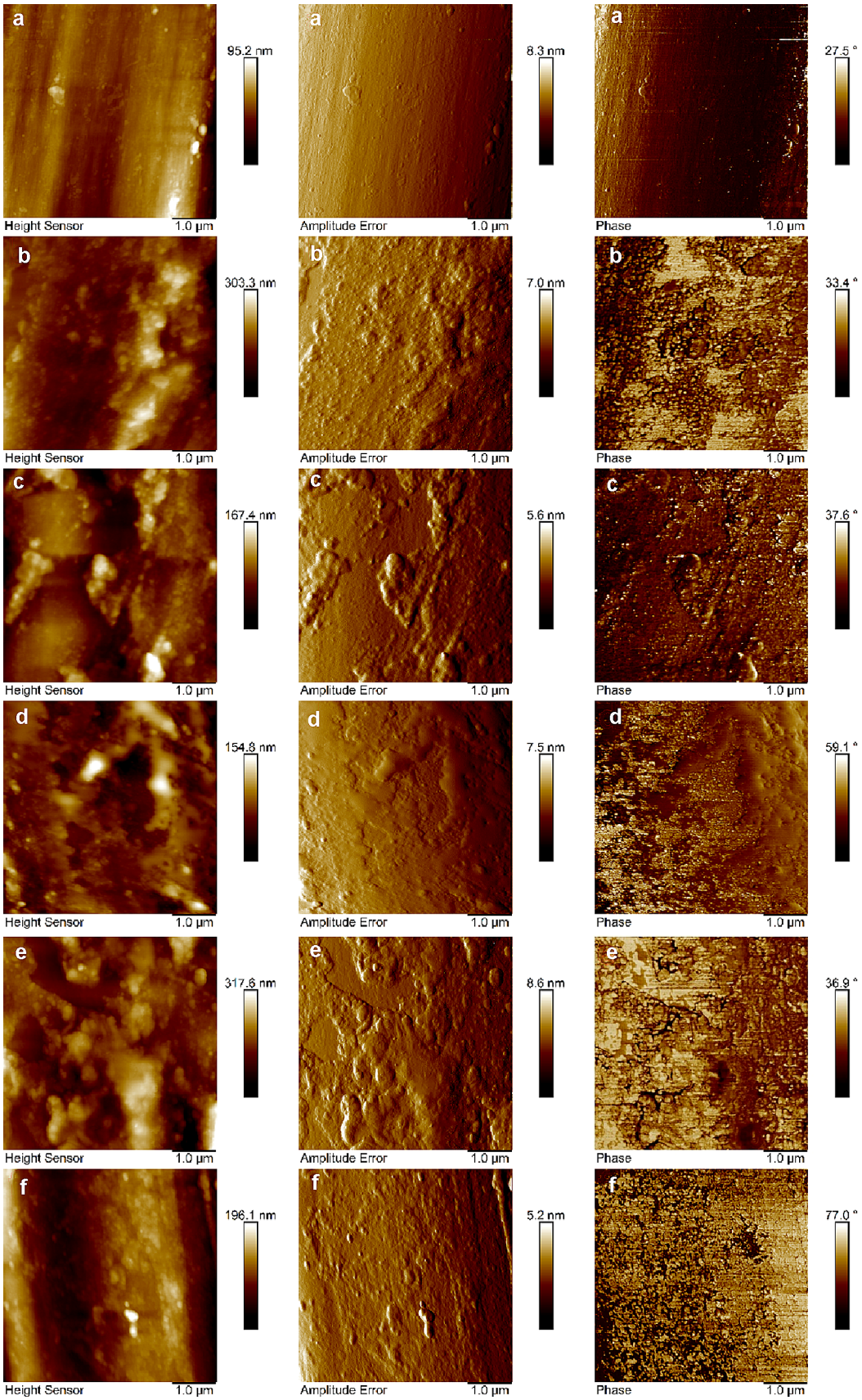
a
95.2 nm
Height Sensor
1.0 µm
a
8.3 nm
Amplitude Error
1.0 µm
a
27.5 °
Phase
1.0 µm
b
303.3 nm
Height Sensor
1.0 µm
b
7.0 nm
Amplitude Error
1.0 µm
b
33.4 °
Phase
1.0 µm
c
167.4 nm
Height Sensor
1.0 µm
c
5.6 nm
Amplitude Error
1.0 µm
c
37.6 °
Phase
1.0 µm
d
154.8 nm
Height Sensor
1.0 µm
d
7.5 nm
Amplitude Error
1.0 µm
d
59.1 °
Phase
1.0 µm
e
317.6 nm
Height Sensor
1.0 µm
e
8.6 nm
Amplitude Error
1.0 µm
e
36.9 °
Phase
1.0 µm
f
196.1 nm
Height Sensor
1.0 µm
f
5.2 nm
Amplitude Error
1.0 µm
f
77.0 °
Phase
1.0 µm

◂**Fig. 3** Atomic force microscopy of untreated fiber and functionalized fiber with dopamine **a** KF, **b** KF-UV(0 h)-PDA, **c** KF-UV(10 h)-PDA, **d** KF-UV(20 h)-PDA, **e** KF-UV(30 h)-PDA, **f** KF-UV(40 h)-PDA)

Table 1 Surface roughness of untreated KF and KF-UV-PDA fibers

Sample	R_q (root mean square roughness)/nm	R_a (arithmrtic mean roughness)/nm
KF	10.7	7.6
KF-UV(0 h)-PDA	19.9	14.9
KF-UV(10 h)-PDA	23.9	18.9
KF-UV(20 h)-PDA	28.3	22.5
KF-UV(30 h)-PDA	43.2	33.5
KF-UV(40 h)-PDA	33.9	29.5

carboxyl functional group on the fiber increased. According to the results of the XPS Fig. 6g, h, compared with KF-UV fiber, KF-UV(40 h)-PDA fiber increased a peak of –OH(286.1 eV) group, which was a characteristic absorption peak of dopamine indicating that dopamine was successfully coated on the surface of the fiber, which was mutually confirmed by the results of SEM and FTIR.

4.6 X-ray Diffraction Analysis (XRD)

It was known from the results of FTIR and XPS that the chemical structure of the surface of the aramid fiber changed after UV radiation and functionalization with dopamine. Then, whether the UV radiation and functionalization with

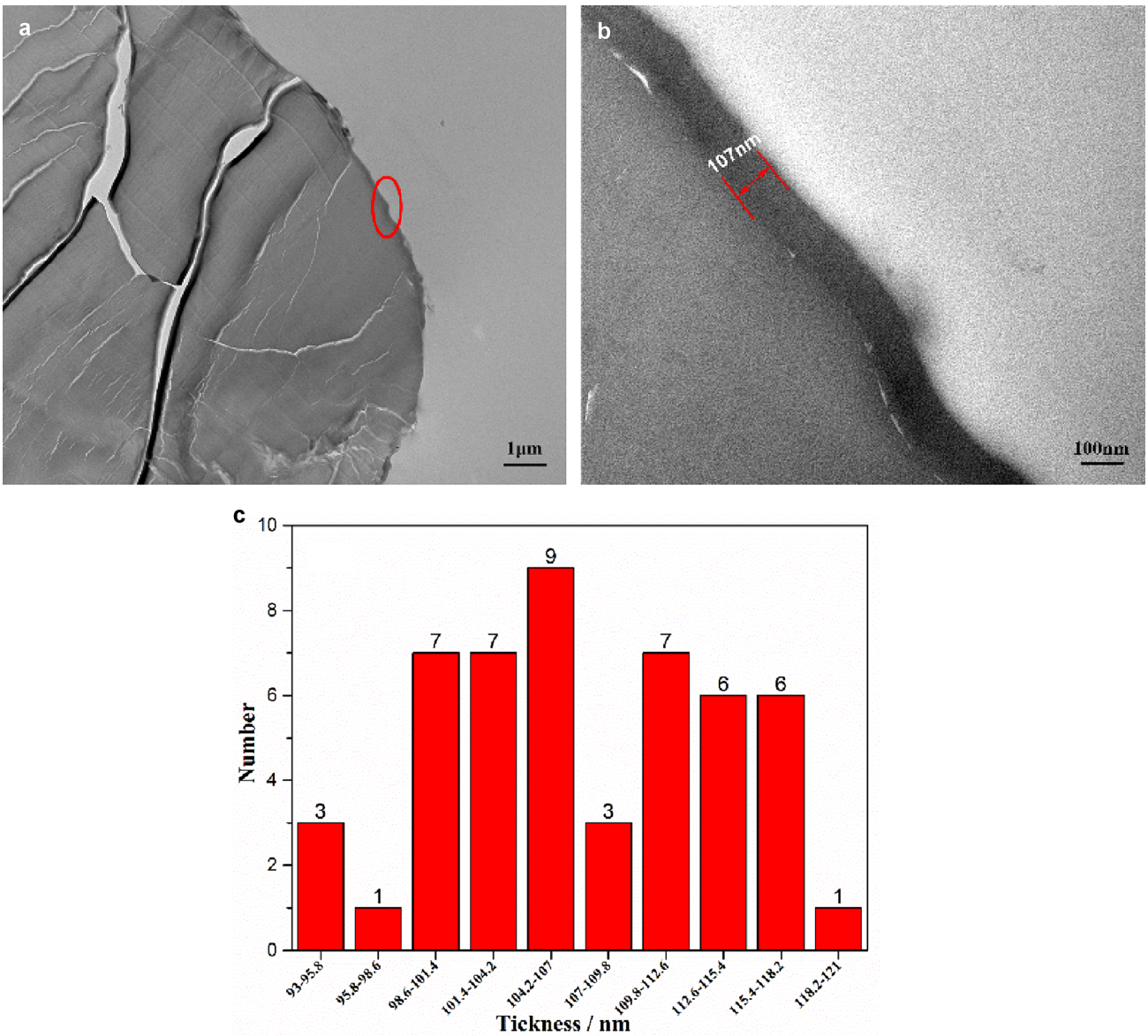

Fig. 4 TEM and the thickness distribution of KF-UV(40 h)-PDA aramid fiber

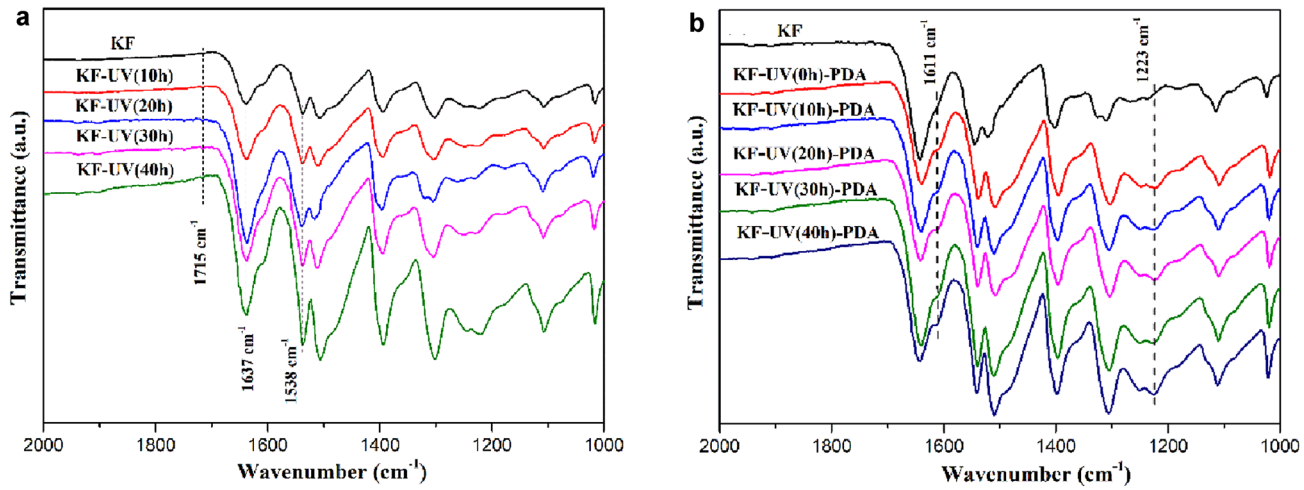

Fig. 5 Infrared spectrum of untreated aramid fiber, modified fiber under UV radiation and functionalized aramid fiber with dopamine

dopamine also changed the aggregation structure of the aramid fiber? So, the X-ray diffraction pattern of the untreated aramid fiber, the UV radiated fiber and the functional fiber with dopamine were carried out, and the results were shown in Fig. 7. As can be seen from the figure, KF-UV-PDA fiber, KF-UV fiber and KF had similar XRD diffraction patterns, which were mainly two sharp diffraction peaks: 2θ were 20.5 and 22.8 corresponding to the characteristics (110) and the (200) crystal plane of aramid fiber, respectively [35, 36]. The results indicated that UV radiation and functionalization with dopamine did not change the aggregation structure of the aramid fiber. However, the UV radiated fiber, the intensity of the characteristic diffraction peak was lower than that of the untreated aramid fiber, indicating that the crystallinity of the UV radiated fiber was lowered. Through the testing, the corresponding crystallinities of KF, KF-UV fiber and KF-UV-PDA fiber were 81.11%, 58.60% and 65.46%, respectively. Because the aramid fiber underwent UV radiation and damaged the surface structure of the fiber, resulting in a decrease in the overall crystallinity. However, the crystallization degree of the functional fiber with dopamine improved, which may be due to the fact that dopamine reacted with the functional groups on the surface of the fiber, improving the regularity of the fiber to a certain extent, so the crystallinity was improved. In summary, the treatment method used in this paper was mild and did not damage to the aggregation structure of aramid fiber.

4.7 Surface Infiltration Performance Analysis

Common contact angles were used to characterize the surface wetting of fibers [36]. Figure 8 showed the contact angle of untreated KF and KF-UV-PDA fibers with deionized water. It can be seen from the figure that KF had the largest contact angle and exhibited hydrophobicity, while as the UV radiation time increased, the contact angle of the fiber became smaller, which indicated that the hydrophilicity of the KF-UV-PDA fibers increased, proving that the surface wettability of KF-UV-PDA fibers was better than KF, especially the KF-UV(40 h)-PDA fiber had the best surface wettability. The reason was more likely that the improvement of the surface wettability was related to the change of the structure of the aramid fiber. After the fiber was functionalized of with dopamine, the hydrophilic active group (hydroxyl group) on the fiber increased, which was confirmed by the FTIR and XPS results.

4.8 Ultraviolet Absorption Spectrum Analysis

Figure 9 showed the UV absorption spectra of KF and KF-UV(40 h)-PDA fibers. It can be clearly seen from Fig. 9 that compared with KF, the absorption intensity of the ultraviolet absorption peak near 217 nm and 305 nm of KF-UV(40 h)-PDA fiber was significantly improved by 106.83%, 57.29%, respectively. What's more, the width of the absorption peak near 305 nm was increased. The reasons for the improvement of the absorption intensity near 217 nm was that the surface of the KF-UV(40 h)-PDA fiber had hydroxyl group (–OH) chromophore in the dopamine, which had a lone pair of electrons, and itself could not absorb light larger than 200 nm. However, when it was connected to the chromophore (double bond in the benzene ring), it could interact with the π electron in the benzene ring, so that the $n \rightarrow \sigma^*$ transition energy was reduced, thereby enhancing its absorption intensity. The reason of the improvement of absorption peak near 305 nm was that after the UV radiation, the hydrogen bond and the amide bond between the molecular chains of the aramid fiber were broken, and

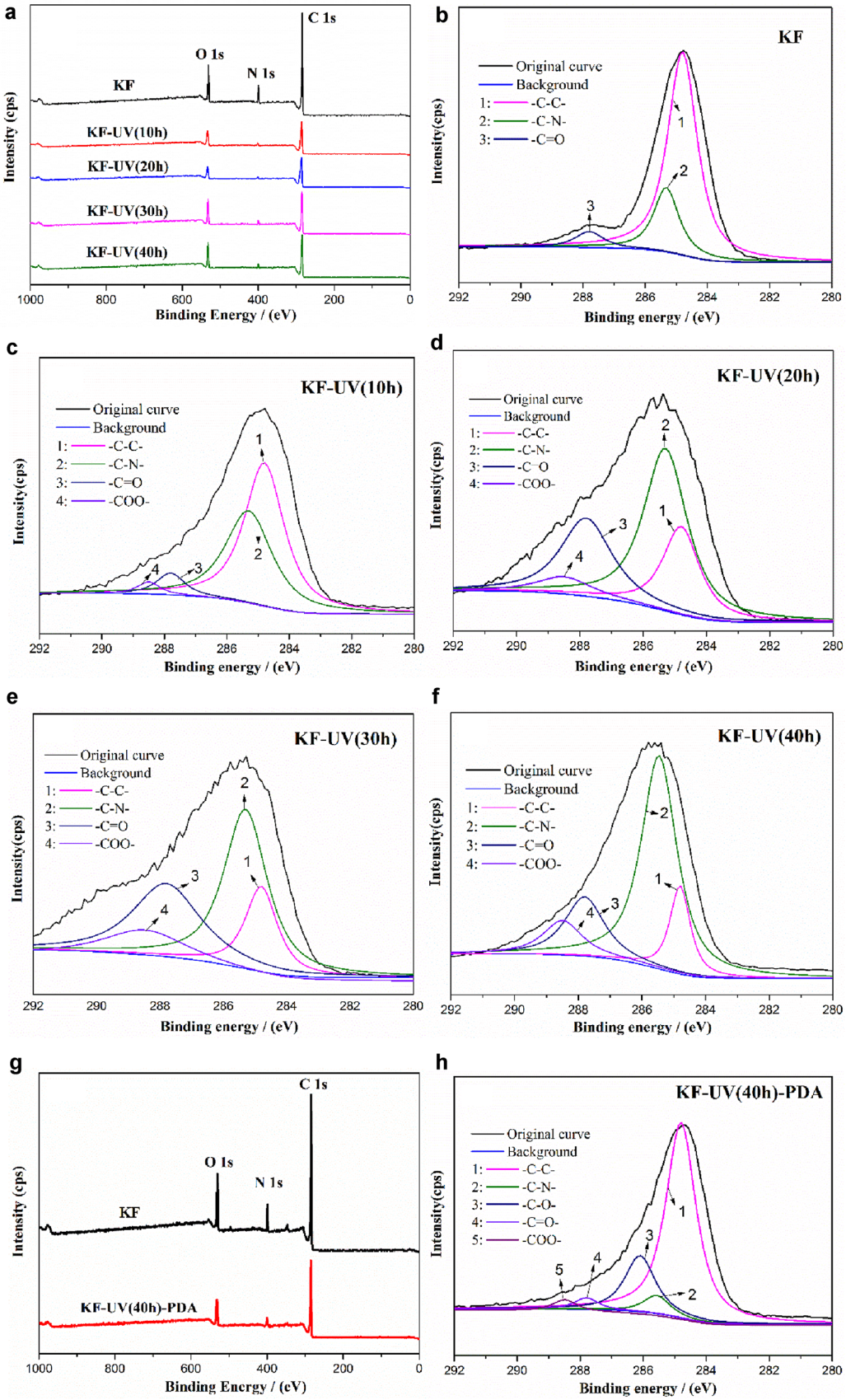

Fig. 6 XPS spectrum of untreated aramid fiber, UV radiated fiber and functionalized fiber with dopamine

Table 2 Chemical composition on the surface of untreated KF, KF-UV(40 h) and KF-UV(40 h)-PDA fiber

Fiber	Chemical composites (atomic%)		
	C	N	O
KF	78.36	7.96	13.67
KF-UV(40 h)	79.25	4.29	16.46
KF-UV(40 h)-PDA	79.51	5.72	14.77

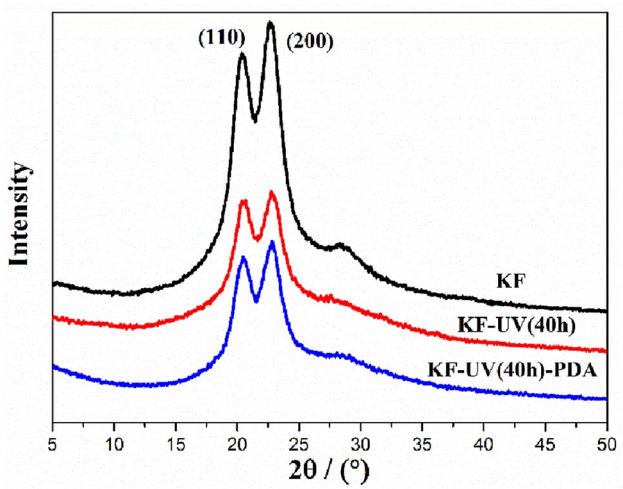

Fig. 7 XRD pattern of KF, KF-UV(40 h) and KF-UV(40 h)-PDA fiber

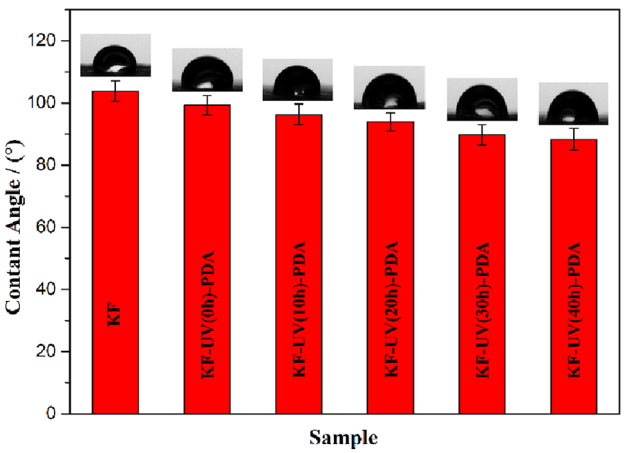

Fig. 8 Contact angle test chart of untreated KF and KF-UV-PDA fibers

then the oxidation of the UV radiation produced carboxyl functional group, which could generate an ester with the hydroxyl group in dopamine. The carbonyl group in the ester and the benzene ring of dopamine could produce conjugated reaction [37], which reduced the transition energy of n → π*, thereby significantly increasing the absorption intensity near

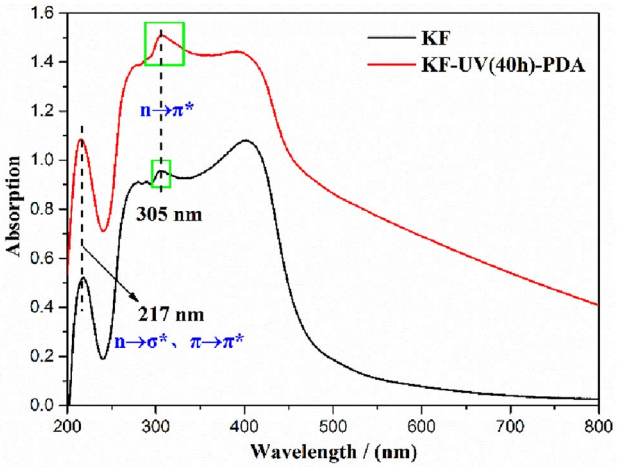

Fig. 9 Ultraviolet absorption spectrum of KF and KF-UV(40 h)-PDA fiber

305 nm. In summary, the functional fiber with dopamine had excellent UV resistance, and the change of the absorption intensity of the absorption peak was closely related to the change of chemical structure on the fiber. Therefore, the ultraviolet absorption spectrum had a great significance for studying the chemical structure of the aramid fiber.

4.9 Analysis of Mechanical Properties

The mechanical properties of KF and KF-UV-PDA fibers were shown in Fig. 10. It can be seen from the figure that as the UV radiation time increased, the strength and elongation at break of the fiber gradually decreased. Compared with KF, the strength and elongation at break of KF-UV(40 h) fiber decreased about 19.15% and 11.26%, respectively. This was because that after the fiber was radiated by UV, defects such as gullies appeared on the surface, where stress concentration tended to occur during the stretching process, which was prone to break, thereby the mechanical properties were lower than the untreated fiber. The strength and elongation at break of KF-UV(40 h)-PDA fiber were reduced by 16.71% and 9.58%, respectively. It was clear that the strength and elongation at break of fiber were improved after functionalization with dopamine. Moreover, compared with KF-UV(40 h) fiber, the strength and elongation at break of KF-UV(40 h)-PDA fibers increased by 2.99% and 3.05%, respectively. This might be the contribution of the dopamine coating on the fiber surface. That was to say, dopamine reacted with the carboxylic acid functional groups on the surface of the fiber to compensate for some of the defects on the fiber. As can be seen from the mechanical data from Fig. 10, the dopamine layer was advantageous for improving the mechanical properties of the fiber.

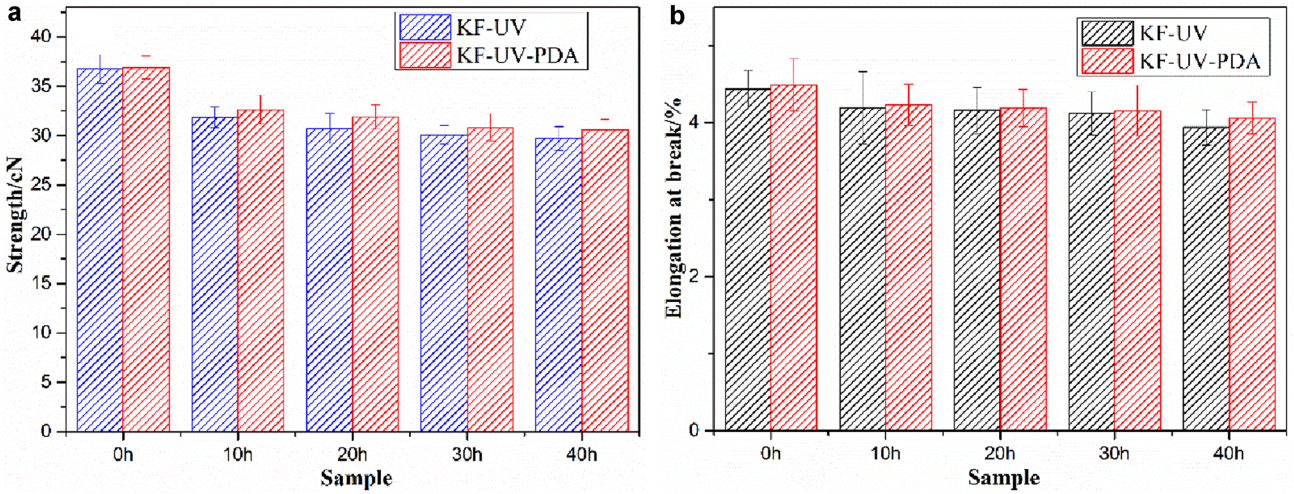

Fig. 10 Mechanical properties of KF and KF-UV-PDA fibers

4.10 Research on the Properties of Fiber after 1 Week of UV Radiation

4.10.1 Scanning Electron Microscopy Analysis

The common testing characterization method against ultraviolet radiation was to observe the surface structure and tensile properties of the fiber. Therefore, KF and KF-UV-PDA fibers after 168 h of UV radiation with SEM and tensile properties were carried out. Figure 11 showed a scanning electron micrograph of aramid fiber after 168 h UV irradiation. It can be clearly seen from the KF diagram that the surface of the fiber became rough, the deep gully appeared in the axial direction of the fiber. The fiber had obvious fracture, the skin layer of the fiber was upwarpped, and deposits were formed on the surface. After the UV radiation of the aramid fiber, the molecular chain was broken, and the terminal group was oxidized. Compared with untreated KF, the surface of KF-UV-PDA fiber was less damaged, and the surface of PDA particles and coating had a small amount of shedding, but the fiber had no gully on the surface. It showed that dopamine could be firmly coated on the surface of the aramid fiber after long time of the UV radiation. The results of the SEM were a good proof that the functionalized fiber with dopamine had an excellent performance of UV resistance.

4.10.2 Analysis of Mechanical Properties

Figure 12 showed the mechanical properties of KF and KF-UV-PDA fibers after 168 h of UV radiation. It can be seen from the Fig. 12 that as the UV irradiation time increased, the strength and elongation at break of the fiber were gradually increased. When the time of UV irradiation was 40 h, the mechanical properties of the sample reached a maximum. It can be seen from the data in the analysis chart that the retention of strength and elongation at break of KF after irradiation for 168 h were only 52.10%, 55.53%. Because after a long period of UV radiation, the fiber was severely damaged, and obvious grooves appeared, where during the stretching process, stress concentration was likely to occur. So that the mechanical properties were seriously degraded. Compared with the untreated fiber, the strength and elongation at break of KF-UV(40 h)-PDA fiber were 75.22% and 74.95%, respectively, which showed a significant improvement in mechanical properties. This fully demonstrated that the PDA layer had excellent UV resistance and can still protect the cortex of the aramid fiber after a long period of ultraviolet radiation.

4.11 Ultrasonic Treatment of KF-UV(40 h)-PDA Fiber

The PDA layer was coated on the fiber evenly and densely, but what about its adhesion? With regards to this, ultrasonic instruments (JP-020, ultrasonic power 120 W, ultrasonic frequency 40KHz, Shenzhen Jiemeng Cleaning Equipment Co., Ltd.) was used for KF-UV(40 h)-PDA fiber for 5 min, 20 min, 40 min and 60 min sonication, and the samples were numbered US-5, US-20, US-40, and US-60, respectively. The SEM images of the obtained fiber were shown in Fig. 13. The adhesion of dopamine was evaluated by observing the degree of shedding of the PDA coating on the surface. It can be clearly seen from the figure that when the KF-UV(40 h)-PDA fiber was treated for 60 min, the PDA coating on the surface had slightly shedding, which fully showed that PDA layer had strong adhesion on the fiber, and had a potential in practical applications.

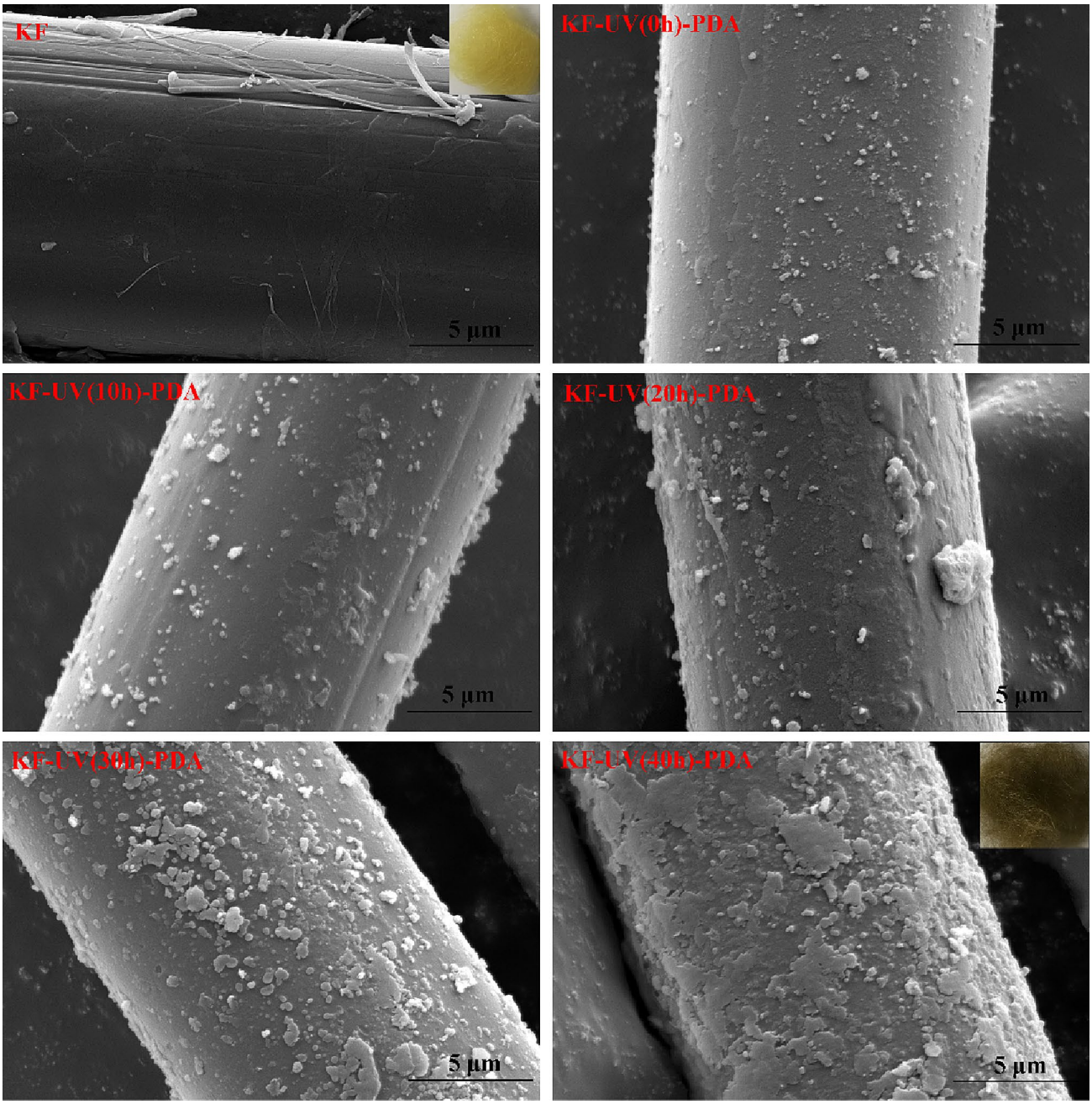

Fig. 11 SEM of KF and KF-UV-PDA fibers after 168 h UV radiation

5 Conclusion

(1) It can be seen from the SEM and AFM images that the surface of the aramid fiber was very smooth. When the aramid fiber was functionalized with dopamine, the coating and particles of dopamine can be clearly seen on the surface of the fiber. Especially for the KF-UV(40 h)-PDA fiber, there was a dense and uniform PDA coating on the fiber, which made the fiber rough. According to the contact angle test, the surface wettability of the functionalized fiber with dopamine was improved, which indicated that the PDA coating increased the surface activity of the fiber. According to the TEM test, the PDA layer was about 107 nm.

(2) It can be seen from the results of the FTIR that after the UV radiation, the chemical structure of the surface changed, the carboxyl group was oxidized to increase the reactive groups on the fiber, which was more advantageous to coat dopamine on the fiber. It was found by XPS results that as the UV irradiation time increased,

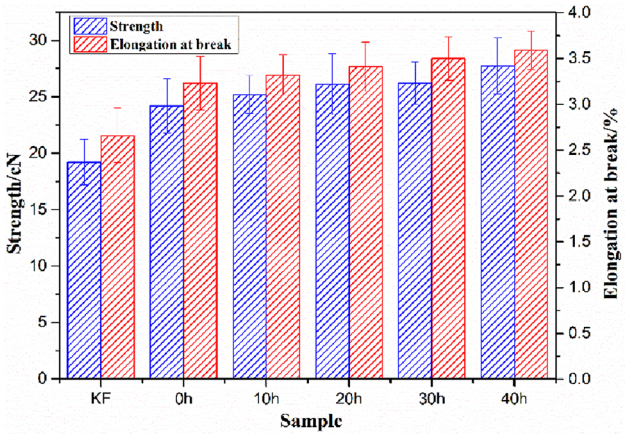

Fig. 12 Mechanical properties of KF and KF-UV-PDA fibers after 168 h UV radiation

the amount of amide bond cleavage increased, and the presence of carboxyl functional groups was further confirmed, which verified that dopamine was successfully coated on the fiber surface. According to the XRD test, the aggregation structure of the fiber did not change after the aramid fiber was functionalized by UV radiation and dopamine.

(3) The UV absorption spectrum was closely related to the structure of the surface of aramid fiber. Corresponding to the absorption peaks around 217 nm and 305 nm, compared with KF, the UV absorption intensity of the functional fiber with dopamine was distinctly enhanced, so the PDA coating had good UV resistance.

(4) KF and KF-UV-PDA fibers were under UV radiation for 168 h, SEM results showed that the PDA coating could protect the cortical structure of aramid fiber very

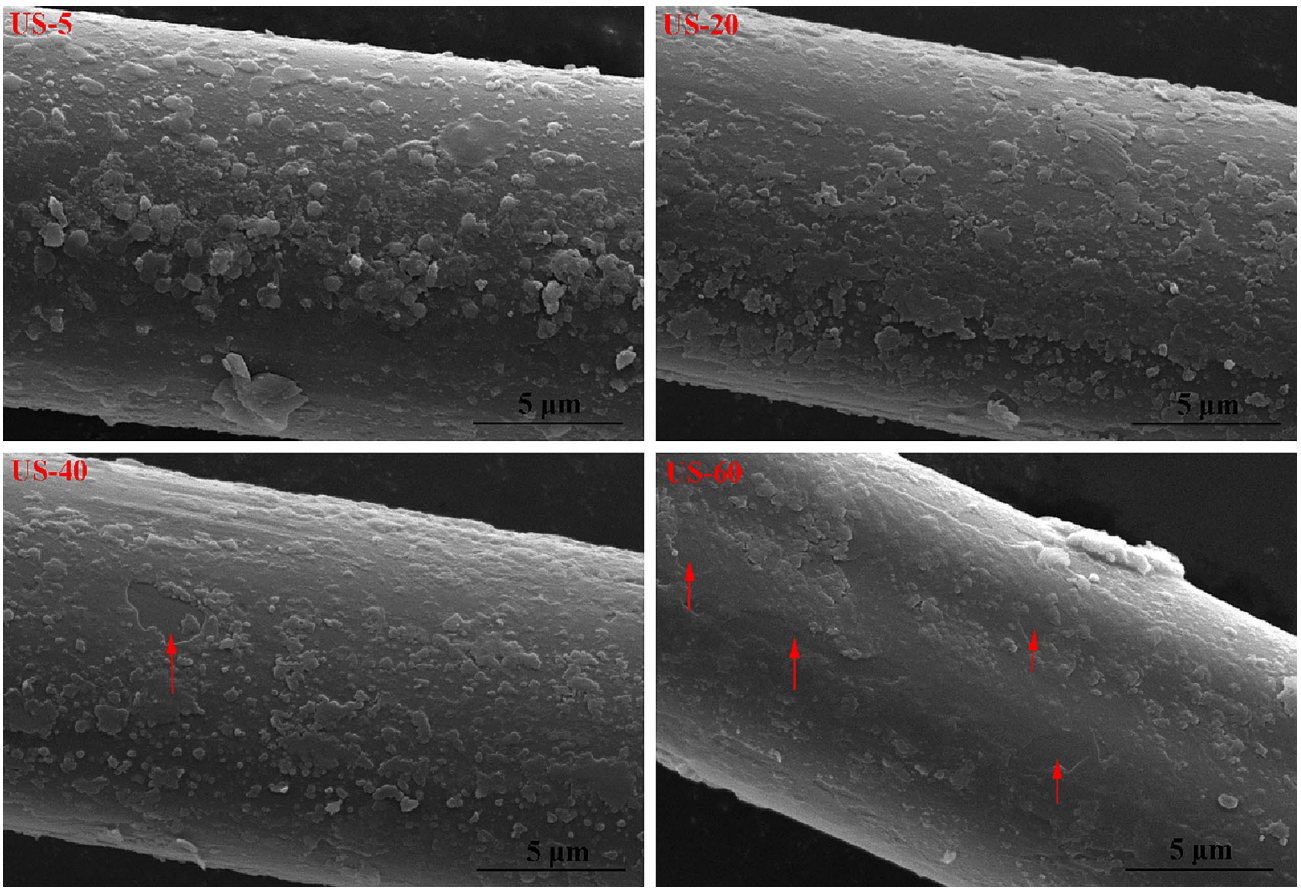

Fig. 13 SEM images of KF-UV(40 h)-PDA fiber after ultrasonic treatment at different times

well. Compared with KF, the mechanical properties test indicated that KF-UV-PDA fiber had high mechanical property retention rate after 168 h UV radiation. Especially for KF-UV (40 h)-PDA fiber, the retention of strength and elongation at break was 23.12% and 19.42% higher than results of the untreated fiber, respectively. This strongly proves that PDA coating has good UV resistance and could increase the service life of aramid fibers. Moreover, the paper provides a novel approach to improve the UV resistance of aramid fibers.

Funding Supported by The Natural Science Foundation of China (No.51563002) and Guizhou Province, "100—level" innovative talents project Qianke Union platform talent [2016] 5653.

References

1. S.H. Zhang, G.Q. He, G.Z. Liang, Comparison of F-12 aramid fiber with domestic armid fiber III on surface feature. Appl. Surf. Sci. **256**(7), 2104–2109 (2010)
2. A.A. Leal, J.M. Deitzel, S.H. Mcknight, Interfacial behavior of high performance organic fibers. Polymer **50**(5), 1228–1235 (2009)
3. P.M. Gore, B. Kandasubramanian, Functionalized aramid fibers and composites for protective applications: a review. Ind. Eng. Chem. Res. **57**(49), 16537–16563 (2018)
4. J.M. García, F.C. García, F. Serna et al., High-performance aromatic polyamides. Prog. Polym. Sci. **35**(5), 623–686 (2010)
5. J. Lin, L. Wang, L. Liu et al., Two-stage interface enhancement of aramid fiber composites: establishment of hierarchical interphase with waterborne polyurethane sizing and oxazolidone-containing epoxy matrix. Compos. Sci. Technol. **193**(16), 108114 (2020)
6. L. Tang, J. Dang, M. He et al., Preparation and properties of cyanate-based wave-transparent laminated composites reinforced by dopamine/POSS functionalized Kevlar cloth. Compos. Sci. Technol. **169**, 120–126 (2019)
7. S. Sharma, J. Rawal, S.R. Dhakate et al., Synergistic bridging effects of graphene oxide and carbon nanotube on mechanical properties of aramid fiber reinforced polycarbonate composite tape. Compos. Sci. Technol. **199**, 108370 (2020)
8. M.O. Seydibeyoglu, A.K. Mohanty, M. Misra, *Fiber Technology for Fiber-Reinforced Composites* (Woodhead Publishing, Cambridge, 2017).
9. Y. Xu, J. Zhu, Z. Wu et al., A review on the design of laminated composite structures: constant and variable stiffness design and topology optimization. Adv. Compos. Hyb. Mater. **1**(3), 460–477 (2018)
10. Y. Guan, W. Li, Y. Zhang et al., Aramid nanofibers and poly (vinyl alcohol) nanocomposites for ideal combination of strength and toughness via hydrogen bonding interactions. Compos. Sci. Technol. **144**, 193–201 (2017)
11. X. Gong, Y. Liu, Y. Wang et al., Amino graphene oxide/dopamine modified aramid fibers: preparation, epoxy nanocomposites and property analysis. Polymer **168**, 131–137 (2019)
12. C. Jia, R. Zhang, C. Yuan et al., Surface modification of aramid fibers by amino functionalized silane grafting to improve interfacial property of aramid fibers reinforced composite. Polym. Compos. **41**(5), 2046–2053 (2020)
13. Y.C. Chu, C.H. Tseng, K.T. Hung et al., Surface modification of polyacrylonitrile fibers and their application in the preparation of silver nanoparticles. J. Inorg. Organomet. Polym. Mater. **15**(3), 309–317 (2005)
14. T.J. Singh, S. Samanta, Characterization of Kevlar fiber and its composites: a review. Mater. Today **2**(4–5), 1381–1387 (2015)
15. C. Cao, J. Peng, X. Liang et al., Strong, conductive aramid fiber functionalized by graphene. Compos. A **140**, 106161 (2021)
16. L.Y. Lei, Y.H. Mao, X.F. Xu, Effect of N, N-diethyl-m-toluamide on the structure and dyeing properties of meta-aramid and para-aramid fibre. Color. Technol. **130**(5), 349–356 (2015)
17. L. Zhou, L. Yuan, Q. Guan et al., Building unique surface structure on aramid fibers through a green layer-by-layer self-assembly technique to develop new high performance fibers with greatly improved surface activity, thermal resistance, mechanical properties and UV resistance. Appl. Surf. Sci. **411**, 34–45 (2017)
18. L. Zhang, H. Kong, M. Qiao et al., Supercritical CO_2-induced nondestructive coordination between ZnO nanoparticles and aramid fiber with highly improved interfacial-adhesion properties and UV resistance. Appl. Surf. Sci. **521**, 146430 (2020)
19. S. Houshyar, R. Padhye, R. Nayak, Deterioration of polyaramid and polybenzimidazole woven fabrics after ultraviolet irradiation. J. Appl. Polym. Sci. **133**(9), 43073 (2016)
20. E.M. Kim, J. Jang, Surface modification of meta-aramid films by UV/ozone irradiation. Fiber. Polym. **11**(5), 677–682 (2010)
21. H. Zhang, G. Liang, A.J. Gu, Facile preparation of hyperbranched polysiloxane-grafted aramid fibers with simultaneously improved UV resistance, surface activity, and thermal and mechanical properties. Ind. Eng. Chem. Res. **53**(7), 2684–2696 (2014)
22. H. Cai, D. Shen, L. Yuan, Developing thermally resistant polydopamine@nano turbostratic BN@CeO_2, double core-shell ultraviolet absorber with low light-catalysis activity and its grafted high performance aramid fibers. Appl. Surf. Sci. **452**, 389–399 (2018)
23. X. Zhu, L. Yuan, G. Liang, Unique surface modified aramid fibers with improved flame retardancy, tensile properties, surface activity and UV-resistance through in situ formation of hyperbranched polysiloxane-$Ce_{0.8}Ca_{0.2}O_{1.8}$ hybrids. J. Mater. Chem. A **3**(23), 12515–12529 (2015)
24. H. Lee, S.M. Dellatore, W.M. Miller, Mussel-inspired surface chemistry for multifunctional coatings. Science **318**(5849), 426–430 (2007)
25. J.H. Ryu, P.B. Messersmith, H. Lee, Polydopamine surface chemistry: a decade of discovery. ACS Appl. Mater. Interfaces **10**(9), 7523–7540 (2018)
26. K.S. Schanze, H. Lee, P.B. Messersmith, Ten years of polydopamine: current status and future directions. ACS Appl. Mater. Interfaces **10**(9), 7521–7522 (2018)
27. J.H. Waite, Mussel power. Nat. Mater. **7**(1), 8–9 (2008)
28. W. Wang, R. Li, M. Tian, Surface silverized meta-aramid fibers prepared by bio-inspired poly(dopamine) functionalization. ACS Appl. Mater. Interfaces **5**(6), 2062–2069 (2013)
29. R.N. Sa, Y. Yan, Z. Wei, Surface modification of aramid fibers by bio-inspired poly(dopamine) and epoxy functionalized silane grafting. ACS Appl. Mater. Interfaces **6**(23), 21730–21738 (2014)
30. S. Li, A.J. Gu, J. Xue, The influence of the short-term ultraviolet radiation on the structure and properties of poly(p-phenylene terephthalaramide) fibers. Appl. Surf. Sci. **265**, 519–526 (2013)
31. H. Zhang, J. Zhang, J. Chen et al., Effects of solar UV irradiation on the tensile properties and structure of PPTA fiber. Polym. Degrad. Stabil. **91**(11), 2761–2767 (2006)
32. Q.Y. Xing, W.W. Pei, R.Q. Xu, *Basic Organic Chemistry*, 4th edn., vol. 1 (Peking University Press, Beijing, 2016).

33. J. Luo, M. Zhang, J. Nie et al., A deep insight into the structure and performance evolution of aramid nanofiber films induced by UV irradiation. Polym. Degrad. Stabil. **167**, 170–178 (2019)
34. R.F. Nascimento, A.O. Silva, R.P. Weber et al., Influence of UV radiation and moisten associated with natural weathering on the ballistic performance of aramid fabric armor. J. Mater. Res. Technol. **9**(5), 10334–10345 (2020)
35. A. Hazarika, B.K. Deka, D.Y. Kim, Growth of aligned ZnO nanorods on woven Kevlar® fiber and its performance in woven Kevlar®fiber/polyester composites. Compos. A **78**, 284–293 (2015)
36. F. Alimohammadi, M.P. Gashti, A. Shamei, Deposition of silver nanoparticles on carbon nanotube by chemical reduction method: evaluation of surface, thermal and optical properties. Superlattice Microstruct. **52**, 50 (2012)
37. H. Chen (ed.), *Analysis, Testing and Research Methods of Polymer Materials* (Chemical Industry Press, 2011)